Picosecond Transient Absorption Spectroscopy in the Blue Spectral Region of Photosystem I†

Dehui Mi, Su Lin, and Robert E. Blankenship*

Department of Chemistry and Biochemistry, Center for the Study of Early Events in Photosynthesis, Arizona State University, Tempe, Arizona 85287-1604

Received May 18, 1999; Revised Manuscript Received August 24, 1999

ABSTRACT: Picosecond transient absorption difference spectroscopy in the blue wavelength region (380−500 nm) was used to study the early electron acceptors in photosystem I. Samples were photosystem I core particles with about 100 chlorophylls per reaction center isolated from the cyanobacterium *Synechocystis* sp. PCC 6803. After excitation at 590 nm at room temperature, decay-associated spectra (DAS) were determined from global analysis in the blue region, yielding two transient components and one nondecaying component. A 3 ps decay phase is interpreted as primarily due to antenna excited-state redistribution. A 28 ps decay phase is interpreted as due to overall excited-state decay by electron transfer. The nondecaying component is ascribed to the difference spectrum of P_{700} and the quinone or A_1 electron acceptor ($P_{700}^+A_1^- - P_{700}A_1$). Decay curves on the millisecond time scale at different wavelengths were measured with an autoxidizable artificial electron acceptor, benzyl viologen, and the ($P_{700}^+ - P_{700}$) difference spectrum was constructed. The ($A_1^- - A_1$) difference spectrum was obtained by taking the difference between the above two difference spectra. A parallel picosecond experiment under strongly reducing conditions was also done as a control experiment. These conditions stabilize the electron on an earlier acceptor, A_0. The nondecaying component of the DAS at low potential was assigned to ($P_{700}^+A_0^- - P_{700}A_0$) since the electron-transfer pathway from A_0 to A_1 was blocked. The [($P_{700}^+A_0^- - P_{700}A_0$) − ($P_{700}^+ - P_{700}$)] subtraction gives a spectrum, interpreted as the ($A_0^- - A_0$) difference spectrum of a chlorophyll *a* molecule, consistent with previous studies. The ($A_1^- - A_1$) spectrum resolved on the picosecond time scale shows significant differences with similar spectra measured on longer time scales. These differences may be due to electrochromic effects and spectral evolution.

Cyanobacteria are oxygenic prokaryotic photosynthetic organisms that contain two distinct photochemical reaction center complexes: photosystem I and photosystem II. Photosystem I is an iron−sulfur type of reaction center which consists of the special pair of chlorophylls, P_{700}, and a series of sequential electron acceptors, all bound to a large integral membrane protein complex along with about 100 antenna chlorophylls. The electron acceptors in this type of reaction center have considerably lower redox potential than those of purple bacteria, green non-sulfur bacteria, and photosystem II. The chemical makeup as well as the energy and electron-transfer processes of photosystem I have been extensively studied (*1*−*3*). The structure of photosystem I from the cyanobacterium *Synechococcus elongatus* has been obtained at 4 Å resolution (*4*, *5*).

The primary electron donor in photosystem I, P_{700}, a pair of chlorophyll molecules, accepts excitations from the antenna pigments. The initial electron transfer is from P_{700}^* to the primary acceptor A_0, also a chlorophyll molecule. From there, the electron is transferred to the secondary acceptor A_1, a molecule of phylloquinone, and on to the iron−sulfur centers F_x and $F_{A/B}$. The initial charge separation from P_{700}^* to form $P_{700}^+A_0^-$ is thought to take 1−2 ps. This is the intrinsic reaction time calculated by assuming the trapping-limited case of antenna dynamics (*6*). In isolated photosystem I, the chlorophyll excited-state lifetime actually observed is longer, about 30 ps, because most of the time the excitation resides on one of the antenna pigments instead of the special pair. This gives rise to an overall antenna decay of about 30 ps, preceded by an energy redistribution phase of about 3 ps (*7*−*9*). Both the special pair and A_0 are thought to be chlorophyll *a* molecules (*10*). The absorption difference spectrum due to ($A_0^- - A_0$) shows the spectral characteristics of (chl a^- − chl *a*) in vitro (*11*−*16*). It is generally accepted that the secondary electron acceptor A_1 is a phylloquinone molecule (*3*, *17*−*26*). The electron transfer from A_0^- to A_1 takes ∼20−30 ps (*16*, *27*). The electron transfer from A_1 to the F_x iron−sulfur (Fe-S) center takes from 15 to 250 ns (*20*, *21*, *28*, *29*), with the longer times found in more intact systems.

The crystal structure of photosystem I from *Synechococcus elongatus* was obtained at 4 Å resolution (*4*), in which the special pair, three Fe-S centers, and four additional chl *a* molecules (the primary acceptor A_0 and its symmetry-related chl *a* called A_0', as well as two accessory chl *a* molecules called A and A′) were clearly revealed. The crystal structure also showed two positions where the electron density map could possibly accommodate the two phylloquinone molecules (A_1 and A_1'), though they are not yet clearly

† This work was supported by NSF Grant MCB-9727607 to R.E.B. This is Publication No. 419 of the Center for the Study of Early Events in Photosynthesis at Arizona State University.

10.1021/bi991139t CCC: $18.00
Published on Web 10/28/1999

distinguishable from aromatic side chains of amino acids. (*4*). The phylloquinones have also been localized by EPR techniques (*19, 30*−*36*). A recent cystallographic study identified the phylloquinone pair and the individual plane orientations of them. One combination of the two chl *a* molecules and the two quinones was found to have the closest correspondence with the pair $P_{700}^{+}A_1^{-}$, based on the comparison of the cystallography data with the EPR data (*5*). Several methods have been developed to extract and reconstitute the two phylloquinones (*22, 37, 38*). Such extraction and reconstitution experiments with either native or non-native quinones provide strong support for the assignment of A_1 as a phylloquinone (*3, 22, 37, 38*). However, both quinones can be extracted and reconstituted with these methods. One quinone is readily extracted without considerable loss of the electron-transfer activity, but the location of this quinone is not established. The available evidence is consistent with the view that only one of the two possible electron-transfer branches is active in photosystem I, but it cannot be ruled out that both of the two potential branches are potentially active (*4, 5, 39*). A symmetric electron-transfer pathway is probably the case in green sulfur bacteria and heliobacteria (*40*, *41*) which also contain an iron−sulfur type of reaction center, but have a symmetric homodimeric protein core inferred to contain two identical electron-transfer pathways.

In this paper, a photosystem II deletion mutant of the cyanobacterium *Synechocystis* sp. PCC 6803, Psb DIC^{-}/DII^{-}, was used (*42*, *43*). The sample is a photosystem I complex with about 100 chlorophyll *a* per RC and also contains carotenoid. The secondary electron acceptor A_1 has no measurable absorbance in the red spectral region where the chlorophylls absorb maximally, so it is necessary to detect it in the near-UV region where it absorbs. First, the difference spectra of ($P_{700}^{+}A_1^{-}$ − $P_{700}A_1$) and of (P_{700}^{+} − P) were obtained. The difference of these two spectra gives what is interpreted to be the difference spectrum of (A_1^{-} − A_1). The ($P_{700}^{+}A_1^{-}$ − $P_{700}A_1$) spectrum was obtained by transient absorption spectroscopy on a picosecond time scale, with 590 nm excitation under neutral redox conditions. The (P_{700}^{+} − P_{700}) spectrum was obtained by transient absorption spectroscopy on a millisecond time scale, using a rapid autoxidizable electron acceptor, benzyl viologen. The (A_1^{-} − A_1) difference spectrum has not been resolved on a picosecond time scale before, although data on the nanosecond time scale are available. As a control, we also did a similar picosecond experiment under strongly reducing conditions, in which electron transfer to A_1 is blocked by prior reduction. This experiment gave what is interpreted to be the (A_0^{-} − A_0) difference spectrum, which agrees well with the known difference spectrum of a chlorophyll *a* molecule.

MATERIALS AND METHODS

Cyanobacterial Growth. A photosystem II deletion mutant of the cyanobacterium *Synechocystis* sp. PCC 6803, Psb DIC^{-}/DII^{-} (*42*, *43*), was used for all experiments. Cells were grown at 30 °C in BG-11 medium in a 12 L glass container, aerated continuously. The medium was prepared from a 100xBG-11 stock, with phosphate, carbonate, and iron. After autoclaving, 5 mM filter-sterilized glucose was added (*9*). The container was illuminated by five 20 W fluorescent tubes placed ∼50 cm from the container. The cells were harvested by continuous flow centrifugation when they turned dark green in 3−4 days.

Sample Preparation. This part of the procedure was carried out at 4 °C. The harvested cells suspended in thylakoid buffer (50 mM HEPES, pH 7, 5 mM $MgCl_2$, 25 mM $CaCl_2$, 10% glycerol, and 0.5% DMSO) were broken into thylakoid membrane fragments by French press treatment at 20 000 psi 3 times. Unbroken cells and large cell debris were removed by centrifugation at 4000 rpm for 4 min in a Sorvall SS-34 rotor. The resultant supernatant liquid was recentrifuged at 16 000 rpm for 20 min to pellet the membrane fragments. The pellet contains the membrane fragments, and the supernatant liquid contains most of the phycobilisomes. The membrane fragments were treated with the detergent, 0.1% β-DM (*n*-dodecyl-β-maltoside), for 5 min and then centrifuged at 8000*g* for 10 min to remove remaining phycobilisomes. The resultant pellet was stirred with 1% β-DM for 1 h to release the photosystem I reaction center complex from the membrane. Centrifugation of the mixture after stirring at 8000*g* for 30 min leaves the photosystem I complex in the supernatant liquid. The complex contains about 100 chlorophylls per reaction center and some carotenoid (*9, 44*).

To prepare samples for picosecond transient absorption spectroscopy, the photosystem I-containing extract was loaded on a sucrose density gradient ranging from 15% to 50% and centrifuged overnight (16 h) at 45000*g*, yielding three bands. The bottom band containing photosystem I trimers was collected (*44*). The sucrose gradient ultracentrifugation was omitted in some experiments with similar results. Samples for experiments under neutral redox conditions were suspended in buffer containing 20 mM Tris-HCl, pH 8.0, 20 mM ascorbate, and 10 μM phenazine methosulfate (PMS) (*9*). For experiments under strongly reducing conditions, samples were suspended in buffer containing 200 mM glycine, pH 11.5, 20 mM ascorbate, 20 μM PMS and then degassed. Sodium dithionite was then added to a final concentration of 30 mM. In both cases, the sample was loaded into a spinning cell with an optical path length of 2.5 mm and a diameter of 18 cm. The absorbance of the sample was adjusted to 1.5−1.6 in the spinning cell at 678 nm, the peak of the Q_y absorption band. The cell was rotated at a speed of 2 revolutions per second.

Spectroscopy. The femtosecond time scale laser system was as previously described (*9*, *45*). The sample was excited at 590 nm with low intensity at room temperature. Briefly, 1064 nm pulses from a mode-locked Nd:YAG laser were compressed, frequency-doubled, and then used to pump a dye laser. The 590 nm output pulses from the dye laser were further compressed to ∼150 fs (fwhm) and amplified to 200 μJ per pulse with a repetition rate of 540 Hz. The amplified pulses were split into two parts: one is the pump beam, and the other beam is further split into the probe and reference beams. The spectra were acquired over a 140 nm wavelength interval on a dual array multichannel detector (Princeton Instruments models DPAA-1024 and ST121) with 0.14 nm per channel. Averaging resulted in a 2 nm interval between data points. Results obtained from global analysis are presented as decay-associated spectra (DAS) (*9*, *16*). In all the measurements, the number of photons absorbed per reaction center was 1 ± 0.1, based on the bleaching

absorption, the sample absorption, and the number of pigments per reaction center complex.

Picosecond absorption difference spectra in the blue spectral region were obtained with a wavelength resolution of 2 nm, in a spectral window of 140 nm (±70 nm from the center wavelength of 450 nm). The integration time for each spectrum was 4 s, during which over 2000 laser flashes were averaged. The repetition frequency of the laser flash was 540 Hz. The time resolution of this series of spectra was 1.2 ps. A total of 100 spectra were taken (from −12 to 108 ps). Each group of 100 spectra was converted to 1 experimental file, and 16 or more such files were averaged. Global analysis was then applied to the averaged file to give decay-associated spectra (DAS).

For the determination of the ($P_{700}^+ - P_{700}$) difference spectrum, the samples were suspended in the same buffer as in the above neutral experiments (pH 8.0) containing about 1 mM ascorbate, 1 μM PMS, and 2 mM benzyl viologen (BV) (*45*). The absorbance of this sample was adjusted to 1.0/cm at 678 nm. A transient absorption spectrophotometer was used for these experiments, as previously described (*46*). The saturating excitation flashes (5 ns fwhm) at 532 nm were provided by the frequency-doubled output of a Nd:YAG laser (Surelite, Continuum). The probe beam was from a tungsten halogen lamp and a monochromator (SPEX 1681). The light transmitted by the sample was focused onto a photomultiplier tube detector (Hamamatsu R-928). A time scale of 100 ms was used, with a delay time between flashes of 5−6 s. A decay curve was obtained at each wavelength by averaging the results of 100 flashes. All these curves were used to construct the ($P_{700}^+ - P_{700}$) spectrum.

RESULTS

Picosecond Experiment in the Blue Region under Neutral Redox Conditions. Samples were prepared, and time-resolved absorption difference spectra were measured as described under Materials and Methods. Spectra were first measured in the 700 nm region and compared to previous data (*16*), in which the nondecaying component has the typical double-negative peaks at 680 and 700 nm. The results agreed very well (data not shown) with results reported in reference *16*.

Figure 1 shows the results of the picosecond spectra in the blue spectral region under neutral redox conditions. Panel A shows the time-resolved spectra at different times. The maximum bleaching is at 440 nm, which decays and blue shifts to 430 nm at later times. A bleaching shoulder at 420 nm also decays and blue shifts to 414 nm. An absorption increase was observed over 450 nm, the center of which evolved from 460 nm to around 470 nm. The 380−400 nm region has a very small negative amplitude. Panel B shows the decay curves at several typical wavelengths. The global analysis reveals three DAS components in panel C. The fastest one (dotted line), a 3 ps decay phase, was attributed to the antenna excitation redistribution process. The 28 ps component (dashed line) was interpreted as due to the overall antenna decay to form $P_{700}^+A_0^-$, as discussed in the introduction. Under these experimental conditions of low excitation intensity, the reduced primary acceptor A_0 decays faster (21 ps) than it forms (28 ps) (*9*, *16*), so there will not be a significant buildup of A_0^-. In this case, the longest,

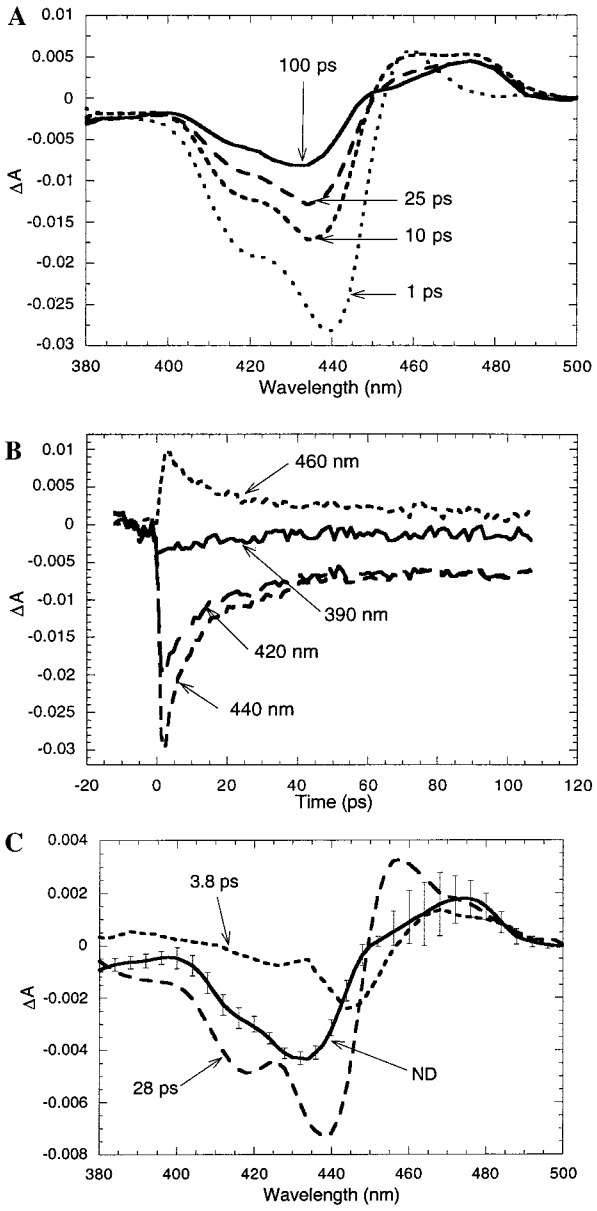

FIGURE 1: Data collected on the picosecond time scale of PSI core particles in the blue wavelength region under neutral conditions at room temperature. (A) Time-resolved spectra. (B) Kinetic traces at several selected wavelengths. (C) Decay-associated spectra. Three components are resolved. ND stands for nondecaying component on this time scale.

nondecaying component (solid line) was attributed to be the difference spectrum of ($P_{700}^+A_1^- - P_{700}A_1$). It can be seen from Figure 1 that the ($P_{700}^+A_1^- - P_{700}A_1$) spectrum has a negative band centered at 430 nm, a shoulder at 414 nm, an isosbestic point at 448 nm, and a positive band around 470 nm with much smaller amplitude. All these features of the nondecaying component are very consistent with the time-resolved spectrum at later times. The ($P_{700}^+A_1^- - P_{700}A_1$) spectrum used to do later subtractions was obtained from the average of five such experiments. These experiments were done on different days with samples prepared in exactly the same way. The error bars in Figure 1 are the standard deviation of the data obtained in the five experiments.

Millisecond Experiment in the Blue Region To Obtain the Difference Spectrum of ($P_{700}^+ - P_{700}$). Experiments were done at room temperature to measure the difference spectrum

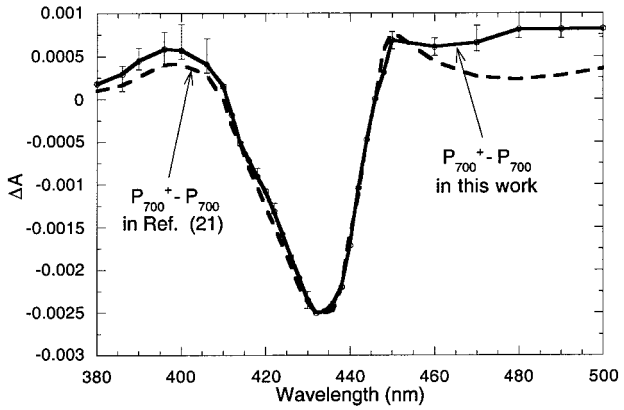

FIGURE 2: ($P_{700}^+ - P_{700}$) spectrum constructed from millisecond experimental data and compared to the same spectrum of *Synechococcus* from reference *21*.

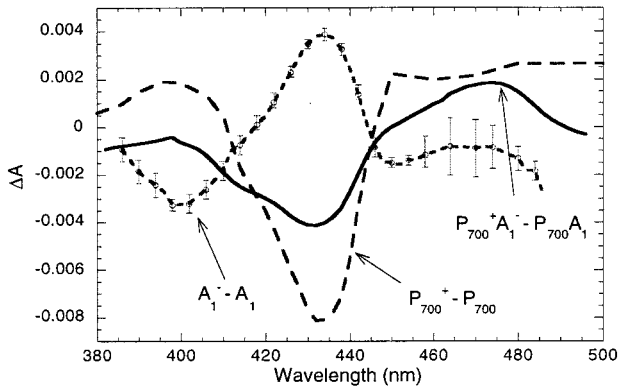

FIGURE 3: Absorption difference spectrum of ($A_1^- - A_1$) obtained on the picosecond time scale by subtracting ($P_{700}^+ - P_{700}$) from ($P_{700}^+A_1^- - P_{700}A_1$).

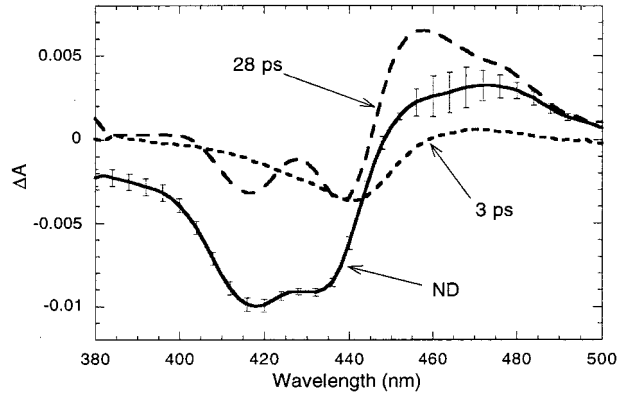

FIGURE 4: Decay-associated spectra on the picosecond time scale of PSI core particles in the blue wavelength region under reducing conditions at room temperature. Three components are resolved. ND stands for nondecaying component on this time scale.

of P_{700} oxidization. To accomplish this, a rapid electron acceptor, benzyl viologen (BV), was added to the sample. The artificial electron acceptor BV can accept electrons from the reduced acceptor (probably $FeS_{A/B}$) and is quickly reoxidized, so that state P_{700}^+ is formed on the millisecond time scale (*46*). Then P_{700}^+ was slowly (2−3 s) re-reduced to the neutral state by the tiny amount of added reductants (ascorbate and PMS) before the next flash. To ensure the recovery of P_{700}^+ before the next flash, the delay time between flashes was 5−6 s. Each decay curve was obtained as an average of 100 or more flashes. The amplitude of the absorbance change at 40 ms after the flash was measured from the decay curve, because at this time the absorbance change is almost entirely due to the ($P_{700}^+ - P_{700}$) contribution, and has no contribution from BV^-. This procedure was carried out at each wavelength from 380 to 500 nm and from 650 to 730 nm with steps of 2 nm. The difference spectrum of ($P_{700}^+ - P_{700}$) versus wavelength was thereby constructed. Each time before spectra were measured in the 400 nm region, a measurement was taken at 700 nm. In the red region (data not shown), the difference spectrum has a negative peak at 700 nm and a broad positive peak beyond 730 nm. Figure 2 shows the ($P_{700}^+ - P_{700}$) spectrum (solid line) in the blue region with a comparison to data from a previous study (*21*). The error bars show the standard deviation of the data. There is a negative band at 430 nm and positive bands above 446 nm and below 410 nm. The negative bands (bleaching) are due to loss of the absorbance of P_{700}, and the increases are due to absorption by P_{700}^+. The band positions and isosbestic points agree well with the ($P_{700}^+ - P_{700}$) spectrum of *Synechococcus* from reference *21*. The two spectra were compared by normalizing at the major bleaching band at 430 nm.

The ($A_1^- - A_1$) Difference Spectrum in the Blue Region under Neutral Redox Conditions. With both the ($P_{700}^+A_1^- - P_{700}A_1$) and ($P_{700}^+ - P_{700}$) spectra available, we can subtract the latter from the former to get a difference difference spectrum which is interpreted as the ($A_1^- - A_1$) spectrum in the blue region. Because these two spectra were measured on different samples at different concentrations and on different machines (see Materials and Methods for details), it is necessary to normalize them before subtraction. The amplitude of the absorption change at 700 nm (ΔA_{700}) of the ($P_{700}^+A_1^- - P_{700}A_1$) spectrum (denoted '*a*') was taken from the nondecaying component of the DAS in the red wavelength region under neutral redox conditions. The ΔA_{700} of the ($P_{700}^+ - P_{700}$) spectrum (denoted '*b*') was taken in the same manner as the other data points used to construct the ($P_{700}^+ - P_{700}$) spectrum. The subtraction was then carried out by calculating ($A_1^- - A_1$) = [($P_{700}^+A_1^- - P_{700}A_1$) − ($P_{700}^+ - P_{700}$)($a/b$)].

Figure 3 shows all three difference spectra. The ($A_1^- - A_1$) spectrum (dotted line) shows a positive band from 416 to 446 nm, centered at 435 nm. There is also a negative bleaching band below 416 nm and a broad decrease above 446 nm, but with lower amplitude. The error bars were obtained in the same way as in Figures 1 and 2.

Picosecond Experiments under Reducing Redox Conditions. This experiment was done in the same way as under neutral redox conditions except with a reduced sample (see Materials and Methods). Under these conditions, the quinone acceptor is stably reduced, most likely as the doubly reduced form. The transient state created, $P_{700}^+A_0^-$, is stable for 35−50 ns (*47*, *48*). The DAS also resolved three components here (Figure 4) with virtually the same lifetimes as those observed under neutral conditions (Figure 1). The first two were considered to be the same processes as those observed under neutral conditions, because reduction is unlikely to affect energy transfer events. The nondecaying component (solid line) was interpreted as the difference spectrum of ($P_{700}^+A_0^- - P_{700}A_0$). Several features of this spectrum can be seen: a broad negative band around 420 nm; a positive band from 446 to 500 nm.

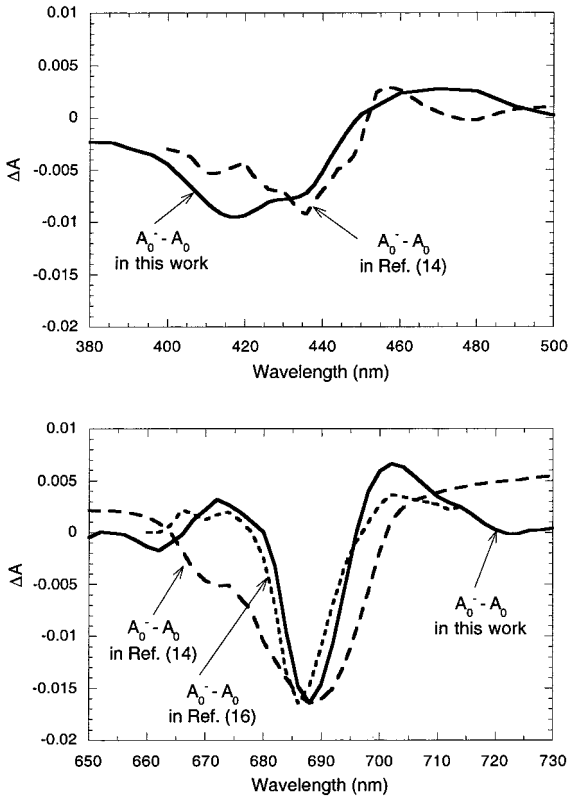

FIGURE 5: Absorption difference spectrum for ($A_0^- - A_0$) resulting from the experiments under reducing conditions (solid lines) compared with the same spectrum in spinach from reference *14* (dashed lines) in both the blue wavelength region (upper panel) and the red wavelength region (lower panel). The lower panel also shows the comparison with the same spectrum from reference *16* (dotted line).

To make sure that dithionite indeed reduces the acceptors as expected, the ($P_{700}^+ - P_{700}$) decay kinetics of the sample on the millisecond time scale were checked on the millisecond spectrophotometer each time before the femtosecond experiment. For a neutral sample, the decay time was over 30 ms, while for a reduced sample with dithionite it was less than 1 ms, which was beyond the resolution of the millisecond machine. Also, picosecond spectra in the 700 nm region were obtained and compared to earlier work that shows a single broad negative peak at 680 nm and a small shoulder around 695 nm (*16*).

The subtraction of ($P_{700}^+ - P_{700}$) from ($P_{700}^+A_0^- - P_{700}A_0$) was carried out to obtain the ($A_0^- - A_0$) difference spectrum in a manner similar to that described above. The ($P_{700}^+ - P_{700}$) millisecond spectrum in Figure 2 was used, and correction was made to account for different ΔA_{700} values of both the picosecond spectrum and the millisecond spectrum. The result is shown in Figure 5 (top panel, solid line). This spectrum was also extended to the red region and compared to results from previous studies (bottom panel, dotted line and dashed line) (*14*, *16*). In the red region, the nondecaying component of the picosecond spectrum under neutral conditions [which is due to only ($P_{700}^+ - P_{700}$) contributions] was subtracted from that under reducing conditions [which is ($P_{700}^+A_0^- - P_{700}A_0$) contributions]. A small correction was made to account for differences in sample concentration. The ($A_0^- - A_0$) difference spectrum has two negative bands, a broader one at 420 nm and another at 688 nm, and the ratio of their amplitudes is 1:(1.6−1.8).

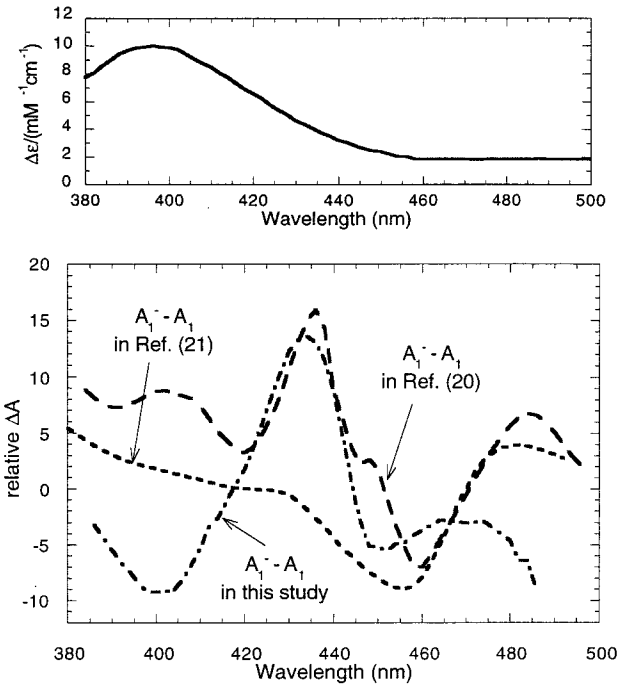

FIGURE 6: The upper panel shows the reduction of vitamin K_1 (PhyQ) to its semiquinone anion in methanol [redrawn from (*20*), as measured by Dr. E. J. Land]. The lower panel shows the ($A_1^- - A_1$) spectrum in this study (dot-dashed line), the ($A_1^- - A_1$) spectrum (dashed line) calculated from the ($P_{700}^+A_1^- - P_{700}A_1$) spectrum, and the ($P_{700}^+ - P_{700}$) spectrum (not shown here), which were redrawn from reference *20*. The lower panel also shows the ($A_1^- - A_1$) spectrum (dotted line) from another study, reference *21*.

Two positive bands were observed: one around 450−500 nm with very small amplitude (one-fourth of the 420 nm negative band) and the other above 696 nm. All these features are very similar to the ($A_0^- - A_0$) difference spectrum of spinach from reference *14* except that the negative band of our ($A_0^- - A_0$) difference spectrum in the blue region is 10 nm or less shifted to the blue and that in the red region is 2 nm shifted to the blue. The ($A_0^- - A_0$) difference spectrum in the red region from reference *16* comes from the same species as ours. It is essentially identical to our spectrum.

DISCUSSION

The ($P_{700}^+A_1^- - P_{700}A_1$) difference spectrum has been resolved in previous studies, but only on much slower time scales. For example, it was obtained at 10 K with $t_{1/2} \approx 150$ μs charge recombination in spinach (*20*). The ($P_{700}^+ - P_{700}$) spectrum of spinach at room temperature was also resolved earlier (*49*). The difference of these two should be the ($A_1^- - A_1$) difference spectrum, although it was not plotted directly in the paper (*20*). The lower panel of Figure 6 shows the ($A_1^- - A_1$) spectrum (dashed line) calculated from the ($P_{700}^+A_1^- - P_{700}A_1$) spectrum and the ($P_{700}^+ - P_{700}$) spectrum (not shown here) which were redrawn from reference *20*. Specifically, the ($A_1^- - A_1$) difference spectrum so obtained is positive in the 430 nm band, around 485 nm, from 340 to 410 nm, around 295 nm, and is probably also positive around 245 nm. It is negative around 455, 325, and 270 nm (our Figure 6, ref *20*).

Both our ($A_1^- - A_1$) difference spectrum (Figure 3) and the spectrum in reference *20* exhibit significant differences

with the ($PhyQ^- - PhyQ$) spectrum in vitro, which is shown in the upper panel of Figure 6. By comparing the ($P_{700}^+A_1^- - P_{700}A_1$) and ($P_{700}^+ - P_{700}$) spectra, we noticed that only from 420 to 440 nm can the ($A_1^- - A_1$) spectrum have an amplitude big enough to be undoubtedly positive, while in the two flanking portions (from 410 to 420 nm, and from 440 to 450 nm), the ($A_1^- - A_1$) difference spectrum has almost zero amplitude. The positive band of this spectrum in vivo (*20*) is not as broad as in the ($PhyQ^- - PhyQ$) spectrum in vitro, and there seem to be significant spectral shifts.

In our ($A_1^- - A_1$) difference spectrum, the negative amplitude extended down to 380 nm, centered at 395 nm. The ($A_1^- - A_1$) difference spectrum has a positive band from 420 to 446 nm, centered at 434 nm, which perhaps can be attributed to an absorption increase due to the reduction of A_1. In some other studies, a positive band is observed at 375 nm (*21*) or 380 nm, although it is difficult to know if this band has the same origin. The difference in band positions between our data and those from other studies was attributed to the effect of different protein environments [our data in *Synechocystis* are all at room temperature, phylloquinone in vitro; (*20*) in spinach at 10 K; and (*21*) in *Synechococcus* at room temperature]. Also, the subtraction we have done for the data in reference *20* is based on the assumption that the ($P_{700}^+ - P_{700}$) spectra at 10 K and at room temperature are the same, since the ($P_{700}^+ - P_{700}$) spectrum at 10 K was not available. This assumption is not strictly correct, so some distortion is to be expected in this spectrum.

For the 450−500 nm region, the previously reported ($A_1^- - A_1$) spectrum does not overlap very well with the ($PhyQ^- - PhyQ$) spectrum in vitro. The in vitro data have an almost constant but very weak positive change here (Figure 6, upper panel), while the spectra derived from references *20* and *21* have both positive and negative features here. The 450−500 nm region in our spectrum has a small negative amplitude (Figure 3). This variation may be due to an electrochromic influence induced by the charge of A_1^-. Some previous data, like reference *21* (shown in our Figure 6, bottom panel), have a large negative band at 450 (from 440 to 470 nm). Considering the fact that oxidized phylloquinone absorbs very weakly above 360 nm, they proposed the electrochromic red shift of a carotenoid may be responsible for this absorbance change (*21*).

As to the 480 nm increase observed in the ($A_1^- - A_1$) spectra in references *20* and *21*, it is observed that our ($P_{700}^+A_1^- - P_{700}A_1$) difference spectrum has its positive band shifted to 470 nm. Since we are subtracting a normalized ($P_{700}^+ - P_{700}$) signal from the ($P_{700}^+A_1^- - P_{700}A_1$) spectrum which has a weak signal/noise ratio, it is not surprising to get the shift of this small positive amplitude here. Also, in reference *20* the data were normalized at a different wavelength. They are based on the assumption that the absorption of P_{700}^+ at 820 nm is identical at 10 K and at room temperature.

There are also other transient ($P_{700}^+A_1^- - P_{700}A_1$) spectra recently resolved with several different photosystem I preparations (*50*−*52*). They all showed the absorption increase somewhere from 350 to 410 nm, but there were variations in the 450−500 nm region, indicating that in this region the spectra are sensitive to the preparation procedure and/or the origin of the samples.

Since we excited the sample at 590 nm, which is far away from the major absorption band of carotenoid (441−482 nm), the carotenoid will not be excited. However, the carotenoid may experience a spectral shift upon charge separation due to an electrochromic effect. Unfortuately, the locations of the carotenoids are not yet resolved in the photosystem I structure.

Our data were quite reproducible. However, there were still some factors leading to possible experimental errors. The picosecond experiments and the millisecond experiments were done with different sample concentrations on different instruments. Also, the sample was not light-saturated (each RC trapped about 1 photon) in the picosecond experiments, while it is saturated in the millisecond experiments. This difference is taken into account by doing the normalization based on ΔA_{700} in both experiments, but does represent a difference in the two experimental designs. The picosecond and millisecond experimental setups and time resolutions were very different, and a large ($P_{700}^+ - P_{700}$) signal is being subtracted from the ($P_{700}^+A_1^- - P_{700}A_1$) spectrum which has a relatively weak signal-to-noise ratio.

An assumption implicit in our experiments is that the ($P_{700}^+ - P_{700}$) difference spectrum measured on the millisecond time scale is the same in the blue region as the ($P_{700}^+ - P_{700}$) difference spectrum measured on the picosecond time scale. Previously, we showed that this is true in the red spectral region, where only the electron donors absorb (*16*) (Figure 5). This gives us some confidence that the ($P_{700}^+ - P_{700}$) spectrum in the blue region is also not time-dependent.

Overall, in this study the ($A_1^- - A_1$) spectrum has been successfully constructed on the picosecond time scale for the first time. After this work was completed, we became aware of a similar study by Brettel and Vos (*53*). The ($A_1^- - A_1$) spectrum was not reported in this reference, but the difference spectrum that they interpret as due to ($P_{700}^+A_1^- - P_{700}A_1$) is generally very similar to our spectrum of the same state, although there are some differences, especially in the wings of the spectrum. In addition, the spectrum interpreted as due to ($P_{700}^+A_0^- - P_{700}A_0$) is similar to our difference spectrum due to phototrapping (27 ps spectrum in Figure 1C), but very different from our ($P_{700}^+A_0^- - P_{700}A_0$) spectrum (ND spectrum in Figure 4), which is obtained under defined redox conditions and verified by parallel measurements in the red spectral region. For these reasons, we think that the 30 ps kinetic phase reported in reference *53* mostly reflects the trapping of excitations, rather than the $A_0^- \rightarrow A_1$ electron-transfer process. However, other work indicates that this electron-transfer process does have approximately this time constant (*13*, *16*, *54*).

ACKNOWLEDGMENT

We thank Dr. Alexander Melkozernov for helpful discussions and Drs. M. Vos and K. Brettel for communicating results prior to publication.

REFERENCES

1. Sétif, P. (1992) in *Topics in Photosynthesis 11. The Photosystems: Structure, Function and Molecular Biology* (Barber, J., Ed.) pp 471−499, Elsevier Science Publishers, Amsterdam.
2. Golbeck, J. M. (1994) in *The Molecular Biology of Cyanobacteria* (Bryant, D. A., Ed.) pp 319−360, Kluwer Academic Publishers, Dordrecht, The Netherlands.

3. Brettel, K. (1997) *Biochim. Biophys. Acta 1318*, 322−373.
4. Schubert, W. D., Klukas, O., Krauss, N., Saenger, W., Fromme, P., and Witt, H. T. (1997) *J. Mol. Biol. 272*, 741−769.
5. Klukas O., Schubert W. D., Jordan, P., Krauss, N., Fromme, P., Witt, H. T., and Saenger, W. (1999) *J. Biol. Chem. 274*, 7361−7367.
6. Trissl, H.-W., Hecks, B., and Wulf, K. (1993) *Photochem. Photobiol. 57*, 108−112.
7. Holzwarth, A. R., Schatz, G., Brock, H., and Bittersmann, E. (1993) *Biophys. J. 64*, 1813−1826.
8. Kumazaki, S., Kandori, H., Petek, H., Ikegami, I., Yoshihara, K., and Ikegami, I. (1994) *J. Phys. Chem. 98*, 10335−10342.
9. Hastings, G., Kleinherenbrink, F. A. M., Lin, S., McHugh, T. J., and Blankenship, R. E. (1994a) *Biochemistry 33*, 3185−3192.
10. Golbeck, J. M., and Bryant, D. A. (1991) *Curr. Top. Bioenerg. 16*, 83−177.
11. Fujita, I., Davis, M. S., and Fajer, J. D. (1978) *J. Am. Chem. Soc. 100*, 6280−6282.
12. Nuijs, A. M., Shuvalov, V. A., van Gorkom, H. J., Plijter, J. J., and Duysens, L. N. M. (1986) *Biochim. Biophys. Acta 850*, 310−318.
13. Shuvalov, V. A., Nuijs, A. M., van Gorkom, H. J., Smit, H. W., and Duysens, L. N. M. (1986) *Biochim. Biophys. Acta 850*, 319−323.
14. Mathis, P., Ikegami, I., and Sétif, P. (1988) *Photosynth. Res. 16*, 203−210.
15. Kim, D., Yoshihara, K., and Ikegami, I. (1989) *Plant Cell Physiol. 30*, 679−684.
16. Hastings, G., Kleinherenbrink, F. A. M., Lin, S., McHugh, T., and Blankenship, R. E. (1994b) *Biochemistry 33*, 3193−3200.
17. Sétif, P., Mathis, P., and Vanngard, T. (1984) *Biochim. Biophys. Acta 767*, 404−414.
18. Mansfield, R. W., and Evans, M. C. W. (1985) *FEBS Lett. 190*, 237−241.
19. Thurnauer, M. C., and Gast, P. (1985) *Photobiochem. Photobiophys. 9*, 29−38.
20. Brettel, K., Sétif, P., and Mathis, P. (1986) *FEBS Lett. 203*, 220−224.
21. Brettel, K. (1988) *FEBS Lett. 239*, 93−98.
22. Biggins, J., and Mathis, P. (1988) *Biochemistry 27*, 1494−1500.
23. Golbeck, J. H. (1992) *Annu. Rev. Plant Physiol. Plant Mol. Biol. 43*, 293−324.
24. Moenne-Loccoz, P., Heathcote, P., MacLachlan, D. J., Berry, M. C., Davis, I. H., and Evans, M. C. W. (1994) *Biochemistry 33*, 10037−10042.
25. Van der Est, A., Bock, C., Golbeck, J., Brettel, K., Setif, P., and Stehlik, D. (1994) *Biochemistry 33*, 11789−11797.
26. Lunberg, J., Fromme, P., Jekow, P., and Schlodder, E. (1994) *FEBS Lett. 203*, 225−229.
27. Hecks, B., Wulf, K., Breton, J., Leibl, W., and Trissl, H.-W. (1994) *Biochemistry 33*, 8619−8624.
28. Mathis, P., and Sétif, P. (1988) *FEBS Lett. 237*, 65−68.
29. Bock, C. H., Van de Est, A. J., Brettel, K., and Stehlik, D. (1989) *FEBS Lett. 247*, 91−96.
30. Bonnerjea, J. R., and Evans, M. C. W. (1982) *FEBS Lett. 148*, 313−316.
31. Gast, P., Swarthoff, T., Ebskamp, F. C. R., and Hoff, A. J. (1983) *Biochim. Biophys. Acta 722*, 163−175.
32. Biggins, J., Tanguay, N. A., and Frank, H. (1989) *FEBS Lett. 250*, 271−274.
33. Biggins, J., Tanguay, N. A., and Frank, H. (1990) in *Current Research in Photosynthesis* (Baltscheffsky, M., Ed.) Vol. 2, pp 639−642, Kluwer Academic Publishers, Dordrecht.
34. Heathcote, P., Hanley, J. A., and Evans, M. C. W. (1993) *Biochim. Biophys. Acta 1144*, 54−61.
35. Heathcote, P., Rigby, S. E. J., and Evans, M. C. W. (1995) in *Photosynthesis: From Light to Biosphere* (Mathis, M., Ed.) Vol. 2, pp 163−166, Kluwer Academic Publishers, Dordrecht.
36. Heathcote, P., Moënne-Loccoz, P., Rigby, S. E. J., and Evans, M. C. W. (1996) *Biochemistry 35*, 6644−6650.
37. Itoh, S., Iwaki, M., and Ikegami, I. (1987) *Biochim. Biophys. Acta 893*, 508−516.
38. Sétif, P., Ikegami, I., and Biggins, J. (1987) *Biochim. Biophys. Acta 894*, 146−156.
39. Schwartz, T., and Brettel, K. (1995) in *Photosynthesis: From Light to Biosphere* (Mathis, M., Ed.) Vol. 2, pp 43−46, Kluwer Academic Publishers, Dordrecht.
40. Büttner, M., Xie, D. L., Nelson, H., Pinther, W., Hauska, G., and Nelson, N. (1992) *Proc. Natl. Acad. Sci. U.S.A. 89*, 8135−8139.
41. Liebl, U., Mockensturm-Wilson, M., Trost, J. T., Brune, D. C., Blankenship, R. E., and Vermaas, W. F. J. (1993) *Proc. Natl. Acad. Sci. U.S.A. 90*, 7124−7128.
42. Vermaas, W. F. J., Williams, J. G. K., and Arntzen, C. J. (1987) *Z. Naturforsch. 42C*, 762−768.
43. Vermaas, W. F. J., Ikeuchi, M., and Inoue, Y. (1988) *Photosynth. Res. 17*, 97−113.
44. Rogner, M., Nixon, P. J., and Diner B. A. (1990) *J. Biol. Chem. 265*, 6189−6196.
45. Lin, S., Chiou, H.-C., Kleinherenbrink, F. A. M., and Blankenship, R. E. (1994) *Biophys. J. 66*, 437−445.
46. Kleinherenbrink, F. A. M., Chiou, H.-C., LoBrutto, R., and Blankenship, R. E. (1994) *Photosynth. Res. 41*, 115−123.
47. Sétif, P., and Bottin, H. (1989) *Biochemistry 28*, 2689−2697.
48. Sétif, P., and Brettel, K. (1990) *Biochim. Biophys. Acta 1020*, 232−238.
49. Ke, B. (1972) *Arch. Biochem. Biophys. 152*, 70−77.
50. Sétif, P., and Brettel, K. (1993) *Biochemistry 32*, 7846−7854.
51. Lüneberg, J., Fromme, P., Jekow, P., and Schlodder, E. (1994) *FEBS Lett. 338*, 197−202.
52. Brettel, K., and Golbeck, J. H. (1995) *Photosynth. Res. 45*, 183−193.
53. Brettel, K., and Vos, M. H. (1999) *FEBS Lett. 447*, 315−317.
54. White, N. T. H., Beddard, G. S., Thorne, J. R. G., Feehan, T. M., Keyes, T. E., and Heathcote, P. (1996) *J. Phys. Chem. 100*, 12086−12099.

BI991139T